NONLINEAR FINITE ELEMENT ANALYSIS OF RESTORING FORCE CHARACTERISTICS OF REINFORCED CONCRETE BEAM-COLUMN JOINTS

Hiroshi Noguchi (I)
Kazuhiro Naganuma (II)
Presenting Author: Kazuhiro Naganuma

SUMMARY

The nonlinear behaviour of reinforced concrete beam-column joints under the reversed cyclic loading was analyzed by the finite element method with the emphasis on the effect of the deterioration factors on the restoring force characteristics of the overall frame. Comparisons were presented with the tests for crack propagation, joint behaviour, bond slips of beam bars through the joint and the restoring force characteristics. From the analysis of the components of the story displacement, the effect of the joint failure and the bond deterioration of beam bars through the joint on the restoring force characteristics was discussed.

INTRODUCTION

In the recent design of reinforced concrete (RC) structures, it is required to ensure the shear strength and ductility of the structural member, such as beams and columns. The high strength and large-sized deformed bar was developed and the dimensions of sections in beams and columns are getting smaller. Consequently the increased ultimate strength of beams and columns yields the high stress state in the beam-column joint. The weak point in the RC frame is going to shift from the constituent members to the joint.

In the previous test results of RC beam-column joints subjected to high-level seismic stresses, the shear cracks in a joint and the slip out of beam longitudinal reinforcing bars through a joint from the bond deterioration were pointed out as the deterioration factors which exerted an undesirable influence upon the restoring force characteristics of RC structures. The effect of these two factors was more remarkable under the reversed cyclic loading than under the monotonic loading in the previous tests, but could not be represented sufficiently by the previous analytical models. Because there are many problems for modelling the nonlinear behaviour such as opening and closing of cracks and crushing of concrete and bond deterioration under the reversed cyclic loading.

In this study, RC cross-type beam-column joints under the reversed cyclic loading were analyzed by the finite element method. The progress of deterioration of the restoring force characteristics was simulated and the effect of the deterioration factors was discussed quantitatively.

(I) Associate Professor, Department of Architectural Engineering, Chiba University, Chiba, Japan

(II) Ohbayashi-gumi Construction Co. Ltd., Tokyo, Japan

MODELLING OF MATERIAL CHARACTERISTICS

In this study, the subject of analysis was limited to the joint without the lateral beams or the eccentric beams, and the plane stress was assumed. The material behaviour was represented as follows.

Concrete

The linearly varying strain triangular element was used for concrete. The nonlinear constitutive law of concrete under bi-axial stresses was based on the modified Darwin's orthotropic model (Ref. 1) and the Kupfer's failure criteria. (Ref. 2) Darwin's model was modified substantially for the rotation of the principal stress axis, because it is very important for the analysis under the reversed cyclic loading. The equivalent uniaxial stress-strain curves, as shown in Fig. 1 were used. The post-crushing behaviour of concrete, the strain-softening portion of the stress-strain curve, was represented by the step-by-step releasing method of the residual stress.

Reinforcing Bars

The longitudinal bar, the stirrup and tie were represented by the bar elements. A simplified bilinear model was used for the stress-strain curve.

Bond Slip

Bond slip was modelled by the bond-link element. Slip characteristics parallel to the bar axis were obtained from the modified bond stress-slip relations under the reversed cyclic loading, as shown in Fig. 2, which were originally proposed by Morita and Kaku. (Ref. 3) As a modified point for Morita's model, when the bond stress yielded the maximum bond strength or the longitudinal bar was yielded, half of the bond stress was released and the bond stiffness was set to zero, as shown in Fig. 2. When the bond failure occurred in both positive and negative directions, the bond stress-slip curve was assumed to be a parallelogram, as shown in Fig. 2. The bond deterioration near the crack was also considered in the proposed model.

Concrete Cracking

In this study, as the crack pattern was predicted from the previous test results, the crack-link element, as shown in Fig. 3, was put in between two nodes on both surfaces of the crack. When the principal stress of a node on the predicted cracking surface exceeded the modulus of rupture, the crack initiation was represented by setting the spring stiffness both vertical and parallel to the crack surface from the initial large values to zero, and crack releasing nodal forces were applied to two nodes across the crack surfaces at the next loading stage. As the effect of the aggregate interlock on the crack surface seemed not to be so great in the joint, it was not considered.

When a crack was closed, the value of the spring stiffness increased gradually as shown in Fig.4. The proposed model represented the following effect of the local contact of crack surfaces; as the slip parallel to the crack surface got larger, the recovery of the spring stiffness got earlier and the local contact effect came to be larger. The reopening of a crack was judged on both accumulative spring force and principal stresses at the

nodes of the crack surfaces.

NONLINEAR ANALYTICAL METHOD

The load incremental method using the tangent modulus was adopted for the nonlinear analysis. At each loading stage, cracking and crushing in concrete and bond failure were checked. The releasing nodal forces caused by the cracking, crushing and bond failure were applied at the next loading stage. The frontal method was used for the solution of the simultaneous, linear algebraic equations.

SPECIMENS FOR SUBJECTS OF ANALYSIS

Three specimens, J-1~3, which were corresponding to the previous cross-type test specimens, were selected for the subjects of analysis. Beam longitudinal bars were arranged through the joint. They were different in the amount of bar arrangement and the material constants. The specimen, J-1, was a joint failure type, and J-2 and J-3 were a beam yielding type. The detailed reinforcement of the specimens and the material constants were shown in Fig. 5 and Table 1 respectively. For specimen J-3, the bond strength and yielding strength of the beam longitudinal bars within the joint were set three times and two times respectively as large as those in J-2 in order to prevent the slip out of beam longitudinal bars from the joint. Therfore, the joint failure and the bond deterioration of beam longitudinal bars for J-1, and the bond deterioration of beam longitudinal bars for J-2, were considered to be dominant as the deterioration factors. It was intended that these deterioration factors were eliminated for J-3.

The finite element idealization of specimen J-1 was shown in Fig. 6. Only half of the whole specimen was analyzed due to the symmetry of the shape and loading condition around a point. The crack pattern was set up using crack-link elements in general accord with the test results under the reversed cyclic loading.

The bond characteristics of longitudinal bars within a joint were given separately in the compression and tension zones, as shown in Fig. 7, in accordance with the previous test results. It was pointed out in the test results of local bond stress-slip curves of beam longitudinal bars that the bond yielding and ultimate bond stress were higher in the compression zone of the joint than in the tension zone. The bond characteristics of longitudinal bars in the beam and column were given in the same way as the compression zone in the joint. The bond strength was reduced near the crack surface because of the bond deterioration.

PROGRESS OF FAILURE

The analytical results were discussed in comparison with the corresponding test results. (Refs. 4 and 5) While specimens J-1 and J-2 were corresponding to the real specimens, J-3 was so idealized model that the analytical results for J-3 were made a comparison with the test results of the most similar specimen. (Ref. 5)

The end of a beam was subjected to the reversed cyclic loading under the constant column axial force. The comparisons of various analytical

cracking and yielding loads with the test results were shown in Table 2. The analytical results gave a good agreement with the test results. The analytical results on the conditions of deformation, crack propagation and concrete crushing for specimen J-1 were shown in Figs. 8 and 9. It was distinguished that concrete crushing occurred on the compression zone and parallel to the diagonal line on the joint surface for J-1.

BEHAVIOUR OF JOINT

The load-joint distortion curves for the analytical model and the test were shown in Fig. 10 for specimens J-1 and J-2. For J-3, the analytical behaviour was about the same as for J-2.

For J-1, the analytical results gave a good match with the test results to the second positive loading. But afterward the increase in the experimental deflection was observed at the time of the negative loading. The joint failure occurred asymmetrically between the positive and negative loading and the failure was remarkable under the negative loading. In the analysis, the shape of loop became slip-typed at the stages from the second negative loading to the third cycle, and it was shown that the concrete deterioration was advanced in the joint. At the third positive loading, the concrete crushing became distinguished parallel to the diagonal line on the joint surface, and cracks were formed in lattices under the reversed cyclic loading.

For J-2 and J-3, the force input into the joint was smaller and the compressive strength of concrete was higher than J-1. So the analytical joint distortion was very small and showed the stable behaviour in the same way as the test results.

BOND SLIP OF BEAM LONGITUDINAL BARS

The bond slips of beam longitudinal bars through the joint were shown in Fig. 11 for specimens J-1 and J-2. For J-3, they were left out from the figure because of much smaller slip in the analysis.

The analytical results obtained a good agreement with the test results for J-1. The slips out from the joint showed a tendency to increase gradually with the increase of loading cycles. This phenominon indicated that the bond deterioration was advanced at the tension side of the joint.

The analytical results for J-2 obtained a good agreement with the test results. It was considered to be due to the bond stiffness degradation from the yielding of beam bars and the bond deterioration of beam bars through the joint that the slips were larger for the lower load in comparison with J-1. It was considered that the bond deterioration of beam bars was caused by pushing the plastic elongation at the tension yielding into the joint under the compression loading. Therfore, the large slips were produced in the stage of the lower load for J-2.

RESTORING FORCE CHARACTERISTICS

The load-story displacement curves were shown in Fig. 12 for specimens, J-1~3.

For J-1 and J-2, the analytical results obtained a good agreement with the test results. In the test for J-3, the local stress concentration occurred in the joint. Consequently the joint failure was caused at the second negative loading, and the analytical results ceased to correspond to the test results.

For J-1 and J-2, the restoring force characteristics changed into the contrary S-type which had the poor energy dissipation capacity, as the cracking in a joint and the bond deterioration of beam reinforcing bars progressed under the subsequent cyclic loading. This tendency was more remarkable for J-2. Meanwhile, the restoring force characteristics were stable spindle-typed.

ANALYSIS OF STORY DISPLACEMENT COMPONENTS

The analytical results of story displacement components at the peak of the positive and negative under each cycle were shown in Fig. 13 for specimens J-1~3.

For J-1, as the loading cycle went on, the components of the joint distortion and the slip out of beam reinforcing bars increased. At the final loading cycle, these components accounted for 50 percent of the story displacement.

For J-2, the components of the column deflection and the joint distortion did not change so much and the value was small. Meanwhile, the component of slip out of beam reinforcing bars increased from the second cycle to the third cycle. At the final, it accounted for about 25 percent of the story displacement. The component of slip out of beam reinforcing bars attained 46 percent of the story displacement just before the yielding of beam bars, and it was proved that its effect on the story displacement was extremely great.

For J-3, the yielding of beam reinforcing bars was dominant. The increse of the story displacement was not so rapid as for J-2. It was shown that the greater part of deflection was the ductile one from the yielding of beam reinforcing bars, and the story displacement was smaller.

From the comparison of the analytical results for three specimens, it could be stated that the beam deflection was constantly stable for J-3, but increased gradually for J-1 and J-2. It was considered that the transformation of the compressive strain of beam bars to tensile strain and the compressive stress concentration near the beam joint from the bond deterioration caused the load compression failure of concrete.

ENERGY DISSIPATION CAPACITIES

The loop shape at each loading cycle and the energy dissipation rate, R_d at every cycle for three specimens J-1~3 were shown in Fig. 14. For J-3, the energy dissipation incresed gradually from the yielding of beam bars, but for J-1 and J-2, the energy dissipation did not increased so much as J-3 because of the gradual deterioration of the loop shape.

CONCLUSIONS

There were many controversial points in the previous analytical models of RC members under the reversed cyclic loading, and especially the unloading stiffness and the hysteresis loop had not been simulated sufficiently.

The analytical results of the model specimens corresponding to the previous test specimens gave a good match with the test results, and it became possible to discuss the deterioration process of the restoring force characteristics and the process of failure in more detail.

It was recognized from this study that the bond deterioration of beam bars would be a primary factor, together with the joint failure, to deteriorate the restoring force characteristics of the overall structures and decrease the flexural yielding strength of beams. From the analytical results on the idealized model which was difficult to be created in the experimental study, it was proved that the prevention of slip out of beam bars through a joint was greatly effective together with the prevention of the joint failure for the improvement of the restoring force characteristics.

REFERENCES

1) Darwin, D. and Pecknold, D.A., "Nonlinear Biaxial Stress-Strain Law for Concrete," Jour. Engr. Mech. Div., ASCE, Vol.103, No.EM2, Apr. 1977, pp.229-241.
2) Kupfer, H.B. and Gerstle, K.H., "Behavior of Concrete under Biaxial Stresses," Jour. Engr. Mech. Div., ASCE, Vol.99, No.EM4, Aug. 1973, pp.853-866.
3) Morita, S. and Kaku, T., "Bond-Slip Relationship under Repeated Loading," Trans. of AIJ, No.229, Mar. 1975, pp.15-24.
4) Kamimura, T. and Hamada, D., et al., "Experimental Study on Reinforced Concrete Beam-Column Joints: Part 1-3," Proc. Annual Conv., AIJ, Sept. 1978, pp.1673-74, Sept. 1979, pp.1303-06.
5) Tada, T., Takeda, T. and Takemoto, Y., "Experimental Study on the Reinforcing Method of RC Beam-Column Joints," Proc. Kanto Dist. Symp., AIJ, July 1976, pp.225-236.

Table 1 Material Properties used for the Analysis

	J-1	J-2・J-3
Concrete	E_c=2.54x10^{5}kgf/cm^2 F_c=-197kgf/cm^2 F_t=29.6 kgf/cm^2 $_b\varepsilon_c$ =0.23%	E_c=2.20x10^{5}kgf/cm^2 F_c=-290kgf/cm^2 F_t=31.7kgf/cm^2 $_b\varepsilon_c$ =0.208%
Longitudinal Bar	SD35 D-22 E_s=1.94x10^{6}kgf/cm^2 σ_y=3633kgf/cm^2	SD30 D-16 E_s=2.11x10^{6}kgf/cm^2 σ_y=3510kgf/cm^2
Stirrup and Tie	SR24 9φ E_{st}=2.11x10^{6}kgf/cm^2 σ_y=3200kgf/cm^2	SR24 9φ E_{st}=1.98x10^{6}kgf/cm^2 σ_y=3300kgf/cm^2

Table 2 Comparisons of Analytical Results with Test Results

	J-1	J-2	J-3
Beam Flexural Crack	1.0(1.3)	1.0(1.5)	1.0(1.5)
Joint Inclined Crack	2.5(3.0)	3.5(4.0)	3.5(4.5)
Beam Bar Yielding	7.2(6.5)	4.6(4.7)	4.5(4.5)
Column Flexural Crack	3.0(3.0)	4.0(3.5)	4.0(3.5)

( )Test Result Unit(tf)

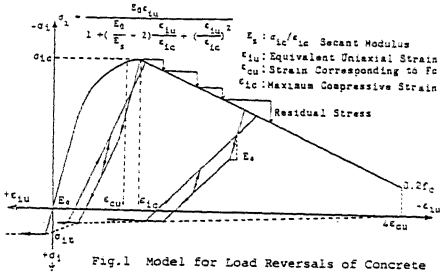

Fig.1 Model for Load Reversals of Concrete

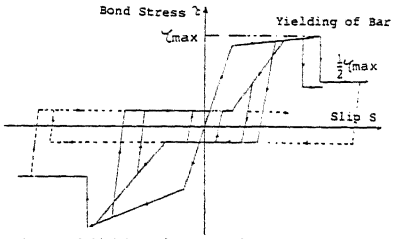

Fig.2 Idelized Bond Stress-Slip Relationships

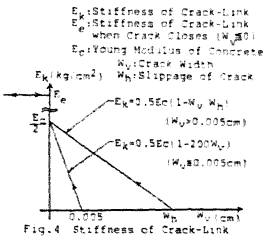

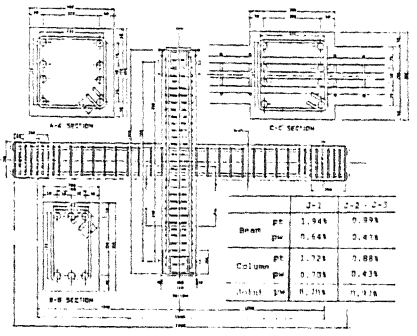

Fig.5 Bar Arrangements of Specimen

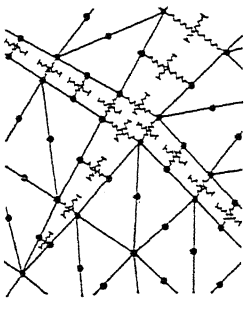

Fig.3 Crack-Linkage Elements

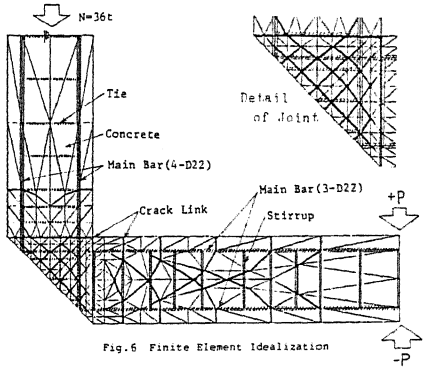

Fig.6 Finite Element Idealization

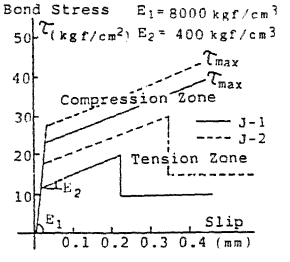

Fig.7 Bond Characteristics of Beam Bars in Joint

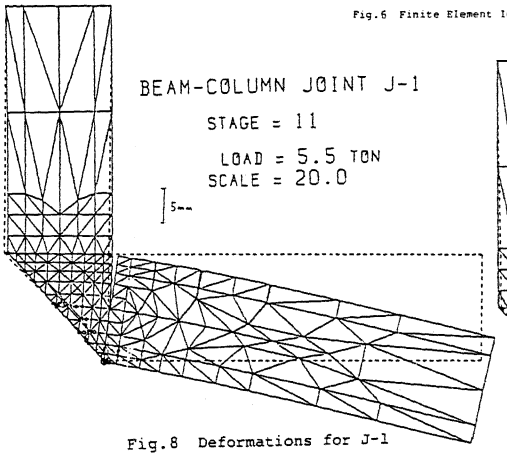

Fig.8 Deformations for J-1

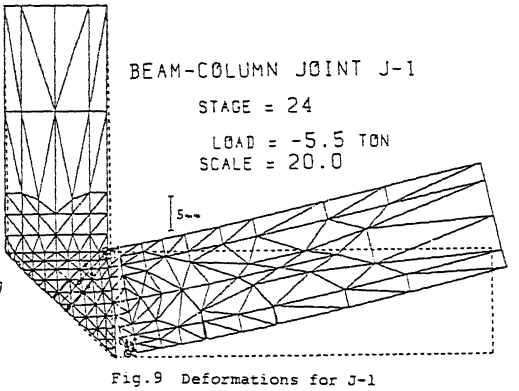

Fig.9 Deformations for J-1

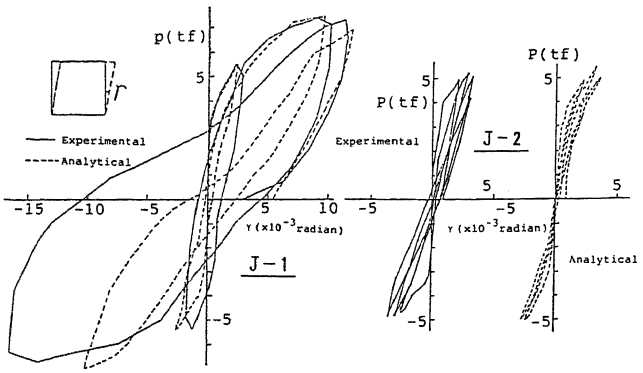

Fig.10 Load-Joint Distortion Relationships

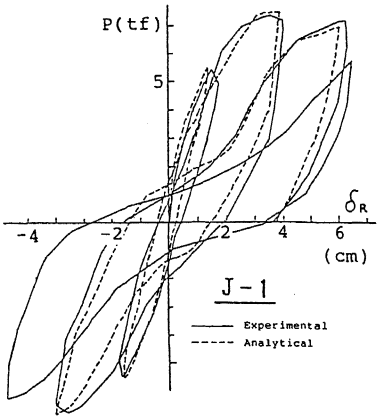

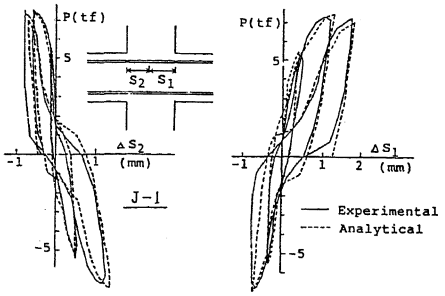

Fig.16 Slips of Beam Bars through Joint

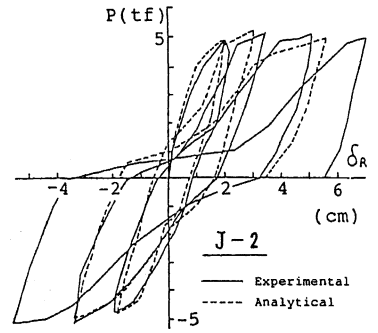

Fig.12 Load-Story Displacement Relationships

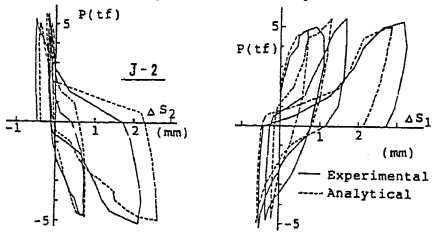

Fig.11 Slips of Beam Bars through Joint

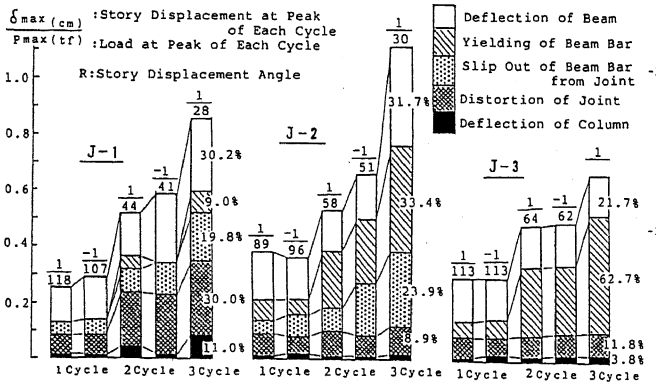

Fig.13 Analysis of Story Displacement Components at Peak of Each Cycle

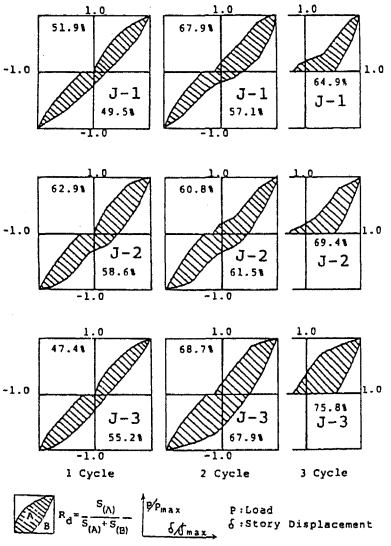

Fig.14 Hysteresis Loop and Energy Dissipation Ratio